OTC OTC-24296-MS

# DESIGN AND MODELING OF FLEXIBLE BALL JOINT PIPE

Thar M. Badri Albarody, and Zahiraniza Mustaffa, Universiti Teknologi PETRONAS, and Mohammed Badri Taufiq, the University of Mustansiriyah.



This paper was prepared for presentation at the Offshore Technology Conference Brasil held in Rio de Janeiro, Brazil, 29–31 October 2013.



## Abstract

Reel-lay process is considered the most efficient installation/construction methods for offshore pipelines and has attracted particular interest on the designing of pipe with large elastic deformation capacity. Therefore, an unbonded, flexible composite ball joints pipe is proposed. The pipe is comprising an internal composite pipe segment with its ball joining to play as liner i.e., carcass, and one or more helical wounding tape stacks applied to the internal liner for absorbing axial and bending loads. The composite tape stacks are formed from a plurality of thin tape strips. All the layers are manufactured from a lightweight composite material consisting of highly noncorrosive epoxied matrix reinforced by long continuous fibers. This paper describes the design parameters of the pipe segments (e.g., modeled as laminated composite cylindrical shell) that form the pipe and its elastic deformations capacity under pure bending conditions (e.g., typical reeling installation condition). To this aim, a straightforward treatment of the problem is presented via using Hamilton's principle and based on the first order shear deformation theories. The solution of the laminated composite cylindrical shell was formulated to follow exactly a simply supported boundary condition. The inter-laminar stresses are evaluated for wide range of orthotropy ratio.

## Introduction

A large diameter, an unbonded, and flexible composite ball joint pipe may be used in particular, although not exclusive, as utility in offshore (e.g., continental shelf environments) or onshore for the transportation of petroleum oil and gas or other fluids. Given that the production of the fossil fuels in offshore fields is limited by a small diameter pipeline was selected to avoid the hydrostatic pressure. It is considered reasonable to assume that the large diameter composite pipes will yield a much higher volume of oil and gas. Thereby the pipe becomes bendable and sufficiently flexible to spool onto reel for the purpose of reeling installation. In general the anti-corrosive and flexible composite pipes are expected to have a lifetime more than 25 years in operation. Flexible pipes are well known in the art and are for example they described in the standards ANSI/API 17 B; Recommended Practice for Flexible Pipe, and ANSI/API 17J; Specification for Unbonded Flexible Pipe. In this paper the proposed flexible ball joint pipe was designed to fulfill a number of requirements:

1. First of all the pipe was designed to have a very high mechanical strength to withstand the forces it will be subjected to during transportation, deploying and in operation.
2. The pipe segments was designed to withstand the internal pressure that are usually considered very high and may vary considerably along the length of the pipe, in particular when applied at varying water depths. Therefore, the pipe segments will design to be stiffer enough to resist the differences in the pressure withstanding the burst and collapse.
3. Simultaneously the flexible pipe was designed from specific composite materials to be highly non-corrosive and chemical resistance.
4. The proposed pipe was designed to keep the weight of the pipe relatively low, both in order to reduce transportation cost and deployment cost but also in order to reduce risk of damaging the pipe during deployment.

Therefore, the present paper will emphases more on the designing of the pipe element to combined the controlled weight (i.e., depending on the buoyancy that required to keep the pipe stable at the design depth) and high strength properties.

## Geometry Description

Assume a flexible pipe is made up of a number of substantially composite pipe elements (i.e., segments attached end to end surrounding a central space), which are inserted outside or interconnected by rigid ball joints. In order to prevent the pipe

elements from becoming detached from each other (i.e., the disassembling of the pipe coupling), the rigid ball joints will provide with four pins on its outer surface, while the pipe elements will provide with a stop hole pressing against the pins. The pipe elements have an accurate surfaces and landings dimension and are maintained in spaced relation allowing the insertion of the rigid ball into its central space maximizing the pipe flexibility. Although the pipe is comprising another element such as: an external thermoplastic fluid-tight cover and one or more helical wounding tape stacks applied to the internal liner for absorbing axial and bending loads, the current research will emphases on the design parameters of the pipe segments only. The rigid pipe elements are found adequate to thick laminated composite cylindrical shell. The cylindrical shell element is assumed to be simply supported which is passable if we considered the ball joint pipe undergo reeling Figure 1.

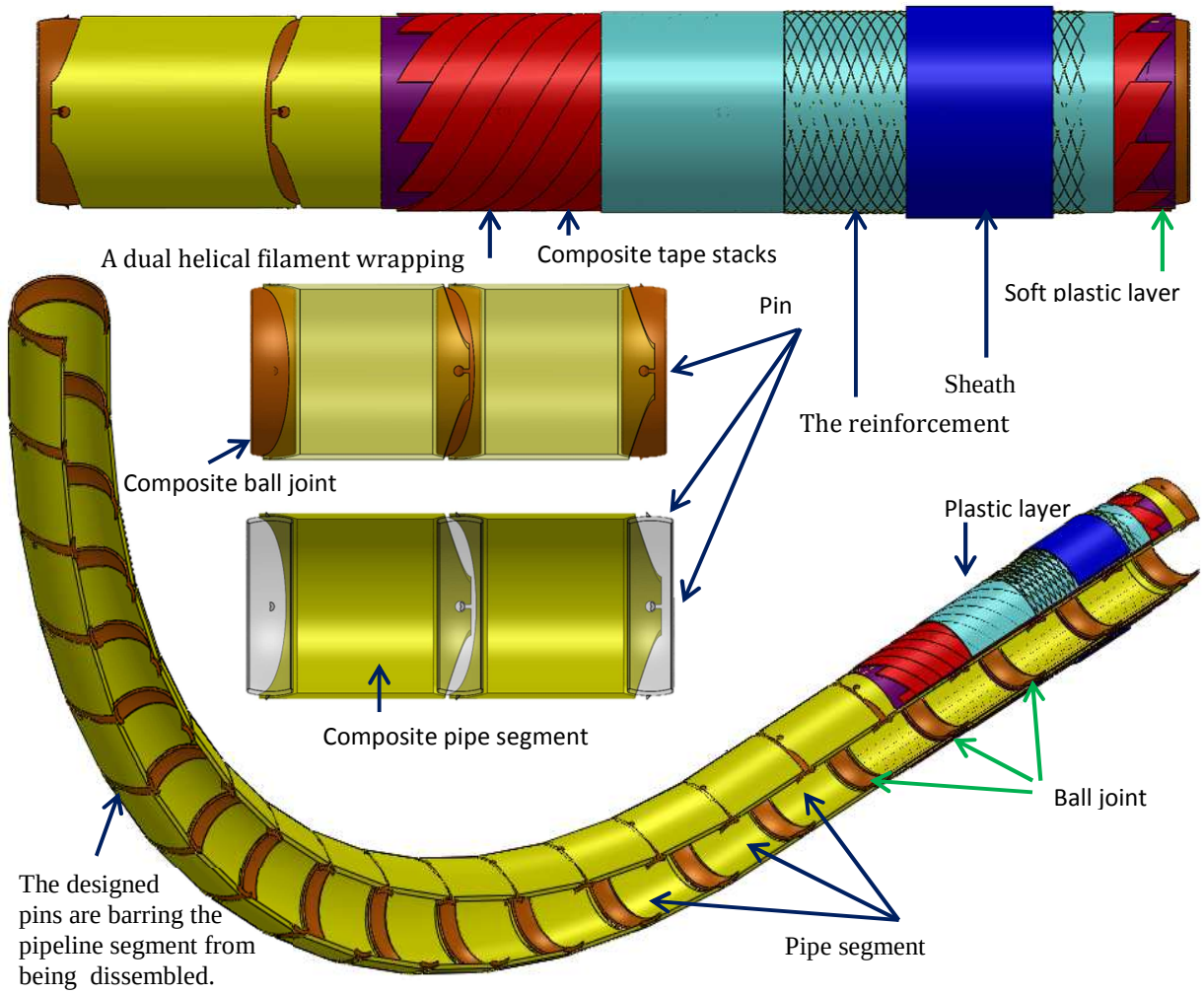


**Figure 1. The flexible ball joint pipe.**

## Kinematic Equations

According to the first-order shear deformation cylindrical shell theory, the following representation of the 3-D displacement field is postulated:

$$\begin{Bmatrix} \varepsilon_\alpha \\ \varepsilon_\beta \\ \varepsilon_{\beta\zeta} \\ \varepsilon_{\alpha\zeta} \\ \varepsilon_{\beta\alpha} \\ \varepsilon_{\alpha\beta} \end{Bmatrix} = \begin{bmatrix} \lambda_\alpha & \cdots & 0 \\ & \lambda_\beta & \\ \vdots & & \\ & \lambda_\beta & \\ & \lambda_\alpha & \vdots \\ & & \lambda_\beta \\ 0 & \cdots & \lambda_\alpha \end{bmatrix} \left( \begin{Bmatrix} \varepsilon_{o\alpha} \\ \varepsilon_{o\beta} \\ \varepsilon_{o\beta\zeta} \\ \varepsilon_{o\alpha\zeta} \\ \varepsilon_{o\beta\alpha} \\ \varepsilon_{o\alpha\beta} \end{Bmatrix} + \zeta \begin{Bmatrix} \varepsilon_{1\alpha} \\ \varepsilon_{1\beta} \\ \psi_\beta / R_\beta \\ \psi_\alpha / R_\alpha \\ \varepsilon_{1\beta\alpha} \\ \varepsilon_{1\alpha\beta} \end{Bmatrix} \right) \quad \text{and} \quad \lambda_\alpha = 1/(1 + \zeta/R_\alpha)$$

where, $u_o$, $v_o$ and $w_o$ are the mid-surface displacements and $\psi_\alpha$ and $\psi_\beta$ are midsurface rotations of the shell. The strains at any point in Codazzi-Gauss shell element can be written as follow:

$$\begin{Bmatrix}\varepsilon_{o\alpha}\\ \varepsilon_{o\beta}\\ \varepsilon_{o\beta\zeta}\\ \varepsilon_{o\alpha\zeta}\\ \varepsilon_{o\beta\alpha}\\ \varepsilon_{o\alpha\beta}\end{Bmatrix}=\begin{bmatrix}\frac{\partial}{\partial\alpha} & 0 & 0 & 0 & 0\\ 0 & \frac{\partial}{\partial\beta} & \frac{1}{R_\beta} & 0 & 0\\ 0 & -\frac{1}{R_\beta} & \frac{\partial}{\partial\beta} & 1 & 0\\ -\frac{1}{R_\alpha} & 0 & \frac{\partial}{\partial\alpha} & 0 & 1\\ \frac{\partial}{\partial\beta} & 0 & 0 & 0 & 0\\ 0 & \frac{\partial}{\partial\alpha} & 0 & 0 & 0\end{bmatrix}\begin{Bmatrix}u_o\\ v_o\\ w_o\\ \psi_\beta\\ \psi_\alpha\end{Bmatrix},\quad \text{and}\quad \begin{Bmatrix}\varepsilon_{1\alpha}\\ \varepsilon_{1\beta}\\ \frac{\psi_\beta}{R_\beta}\\ \frac{\psi_\alpha}{R_\alpha}\\ \varepsilon_{1\beta\alpha}\\ \varepsilon_{1\alpha\beta}\end{Bmatrix}=\begin{bmatrix}0 & 0 & 0 & 0 & \frac{\partial}{\partial\alpha}\\ 0 & 0 & 0 & \frac{\partial}{\partial\beta} & 0\\ 0 & \frac{1}{R_\beta} & -\frac{\partial}{\partial\beta} & 0 & 0\\ 0 & 0 & -\frac{\partial}{\partial\alpha} & 0 & 0\\ 0 & 0 & 0 & 0 & \frac{\partial}{\partial\beta}\\ 0 & 0 & 0 & \frac{\partial}{\partial\alpha} & 0\end{bmatrix}\begin{Bmatrix}u_o\\ v_o\\ w_o\\ \psi_\beta\\ \psi_\alpha\end{Bmatrix}.$$

## Kinetic Equations

Integrating the stresses over the shell thickness, the force and moment resultants will be

$$\begin{Bmatrix}N_\alpha^S\\ N_\beta^S\\ Q_\beta^S\\ Q_\alpha^S\\ N_{\alpha\beta}^S\\ N_{\beta\alpha}^S\\ M_\alpha^S\\ M_\beta^S\\ P_\beta^S\\ P_\alpha^S\\ M_{\alpha\beta}^S\\ M_{\beta\alpha}^S\end{Bmatrix}=\begin{bmatrix}\bar{\varsigma}_{11}^1 & \varsigma_{12}^1 & \varsigma_{14}^1 & \bar{\varsigma}_{15}^1 & \bar{\varsigma}_{16}^1 & \varsigma_{16}^1 & \bar{\varsigma}_{11}^2 & \varsigma_{12}^2 & \varsigma_{14}^2 & \bar{\varsigma}_{15}^2 & \bar{\varsigma}_{16}^2 & \varsigma_{16}^2\\ & \bar{\varsigma}_{22}^1 & \tilde{\varsigma}_{24}^1 & \varsigma_{25}^1 & \varsigma_{26}^1 & \tilde{\varsigma}_{26}^1 & \varsigma_{12}^2 & \tilde{\varsigma}_{22}^2 & \tilde{\varsigma}_{24}^2 & \varsigma_{25}^2 & \varsigma_{26}^2 & \tilde{\varsigma}_{26}^2\\ & & \tilde{\varsigma}_{44}^1 & \varsigma_{45}^1 & \varsigma_{46}^1 & \tilde{\varsigma}_{46}^1 & \varsigma_{14}^2 & \tilde{\varsigma}_{24}^2 & \tilde{\varsigma}_{44}^2 & \varsigma_{45}^2 & \varsigma_{46}^2 & \tilde{\varsigma}_{46}^2\\ & & & \bar{\varsigma}_{55}^1 & \bar{\varsigma}_{56}^1 & \varsigma_{56}^1 & \varsigma_{15}^2 & \varsigma_{25}^2 & \varsigma_{45}^2 & \bar{\varsigma}_{55}^2 & \bar{\varsigma}_{56}^2 & \varsigma_{56}^2\\ & & & & \bar{\varsigma}_{66}^1 & \varsigma_{66}^1 & \varsigma_{16}^2 & \varsigma_{26}^2 & \tilde{\varsigma}_{46}^2 & \varsigma_{56}^2 & \bar{\varsigma}_{66}^2 & \tilde{\varsigma}_{66}^2\\ & & & & & \tilde{\varsigma}_{66}^1 & \varsigma_{16}^2 & \varsigma_{26}^2 & \tilde{\varsigma}_{46}^2 & \varsigma_{56}^2 & \bar{\varsigma}_{66}^2 & \tilde{\varsigma}_{66}^2\\ & & & & & & \bar{\varsigma}_{11}^3 & \varsigma_{12}^3 & \varsigma_{14}^3 & \bar{\varsigma}_{15}^3 & \varsigma_{16}^3 & \tilde{\varsigma}_{26}^3\\ & & & & & & & \tilde{\varsigma}_{22}^3 & \tilde{\varsigma}_{24}^3 & \varsigma_{25}^3 & \varsigma_{26}^3 & \tilde{\varsigma}_{46}^3\\ & & & & & & & & \tilde{\varsigma}_{44}^3 & \varsigma_{45}^3 & \varsigma_{46}^3 & \tilde{\varsigma}_{56}^3\\ & & & & & & & & & \bar{\varsigma}_{55}^3 & \bar{\varsigma}_{56}^3 & \varsigma_{56}^3\\ & & & & & & & & & & \bar{\varsigma}_{66}^3 & \varsigma_{66}^3\\ & & & & & & & & & & & \tilde{\varsigma}_{66}^3\end{bmatrix}\begin{Bmatrix}\varepsilon_{o\alpha}\\ \varepsilon_{o\beta}\\ \varepsilon_{o\beta\zeta}\\ \varepsilon_{o\alpha\zeta}\\ \varepsilon_{o\alpha\beta}\\ \varepsilon_{o\beta\alpha}\\ \varepsilon_{1\alpha}\\ \varepsilon_{1\beta}\\ \varepsilon_{1\beta\zeta}\\ \varepsilon_{1\alpha\zeta}\\ \varepsilon_{1\alpha\beta}\\ \varepsilon_{1\beta\alpha}\end{Bmatrix}$$

*Symmetric*

where $\varsigma_{ij}^p \to p = 1,2,3,4$; is the stiffness properties and the superscript indicate to understand the differences between the extensional, extensional-bending and bending stiffness coefficients, which are defined as follows:

$$\underbrace{\left(\varsigma_{ij}^1,\varsigma_{ij}^2,\varsigma_{ij}^3,\varsigma_{ij}^4\right)}_{(i,j=1,2,6)}=\sum_{k=1}^{N}\int_{h_{k-1}}^{h_k}\hat{\varsigma}_{ij}^k\,(1,\zeta,\zeta^2,\zeta^3)\,d\zeta,\quad \underbrace{\left(\varsigma_{ij}^1,\varsigma_{ij}^2,\varsigma_{ij}^3,\varsigma_{ij}^4\right)}_{(i,j=4,5)}=K_i^2\sum_{k=1}^{N}\int_{h_{k-1}}^{h_k}\hat{\varsigma}_{ij}^k\,(1,\zeta,\zeta^2,\zeta^3)\,d\zeta,\quad and \text{ all other } \varsigma\equiv 0$$

where $[\bar{*}]_{ij}^n=[*]_{ij}^n-C_o[*]_{ij}^{n+1}$ and $[\tilde{*}]_{ij}^n=[*]_{ij}^n+C_o[*]_{ij}^{n+1}$and $\hat{\varsigma}_{ij}^k$ is the transformed properties of orthotropic materials. This method gives a solution for the same choice of deep shell stiffness coefficient, also $K_i$ and $K_j$ are shear correction coefficients, typically taken at 5/6 (Timoshenko 1921). In addition, $h_k$ is the distance from the mid-surface to the surface of the $k^{th}$ layer having the farthest ζ-coordinate.

## Equations of Motion

Based on the laminated composite thick cylindrical shell theories [1] the equations of motion could be drawn as:

$$\frac{\partial}{\partial\alpha}N_\alpha+\frac{\partial}{\partial\beta}N_{\beta\alpha}+\mathcal{F}_\alpha=\left(\bar{I}_1\frac{\partial^2u_o}{\partial t^2}+\bar{I}_2\frac{\partial^2\psi_\alpha}{\partial t^2}\right),\qquad \frac{\partial}{\partial\beta}N_\beta+\frac{\partial}{\partial\alpha}N_{\alpha\beta}+\frac{Q_\beta}{R_\beta}+\mathcal{F}_\beta=\left(\bar{I}_1\frac{\partial^2v_o}{\partial t^2}+\bar{I}_2\frac{\partial^2\psi_\beta}{\partial t^2}\right)$$

$$-\frac{N_\beta^S}{R_\beta}+\frac{\partial}{\partial\alpha}Q_\alpha+\frac{\partial}{\partial\beta}Q_\beta+\mathcal{F}_n=\left(\bar{I}_1\frac{\partial^2w_o}{\partial t^2}\right)$$

$$\frac{\partial}{\partial\alpha}M_\alpha+\frac{\partial}{\partial\beta}M_{\beta\alpha}-Q_\alpha+\mathcal{C}_\alpha=\left(\bar{I}_2\frac{\partial^2u_o}{\partial t^2}+\bar{I}_3\frac{\partial^2\psi_\alpha}{\partial t^2}\right),\qquad \frac{\partial}{\partial\beta}M_\beta+\frac{\partial}{\partial\alpha}M_{\alpha\beta}-Q_\beta+\mathcal{C}_\beta=\left(\bar{I}_2\frac{\partial^2u_o}{\partial t^2}+\bar{I}_3\frac{\partial^2\psi_\beta}{\partial t^2}\right).$$

Having applied the Navier' solution [2], the equations of motion can be written in terms of displacements as $\left(\mathcal{K}_{ij}+\lambda^2\mathcal{M}_{ij}\right)\{\Delta\}=\{\mathcal{F}\}$. Where $\mathcal{K}_{ij}$ is the stiffness matrix and $\mathcal{M}_{ij}$ is the mas matrix, $\{\mathcal{F}\}$ is the applied force, $\{\Delta\}^t=\left\{U_{mn},V_{mn},W_{mn},\Psi_{mn}^\alpha,\ \Psi_{mn}^\beta\right\}$, and $\lambda^2$ is the eigenvalue of the problem. The configuration of the $\bar{\mathcal{K}}_{ij}$ terms for the SS, cross-ply and rectangular plane form is listed below

$$\mathcal{K}_{11}=-\bar{\varsigma}_{11}^1\alpha_m^2-\tilde{\varsigma}_{66}^1\beta_n^2,\ \mathcal{K}_{12}=-(\varsigma_{12}^1+\varsigma_{66}^1)\alpha_m\beta_n,\ \mathcal{K}_{22}=-\tilde{\varsigma}_{22}^1\beta_n^2-\bar{\varsigma}_{66}^1\alpha_m^2-\frac{\tilde{\varsigma}_{44}^1}{R_\beta},\qquad \mathcal{K}_{13}=\left(\frac{\varsigma_{12}^1}{R_\beta}\right)\alpha_m,$$

$$\mathcal{K}_{23}=\left(\frac{\tilde{\varsigma}^1_{22}+\tilde{\varsigma}^1_{44}}{R_\beta}\right)\beta_n\,,\quad \mathcal{K}_{33}=-\tilde{\varsigma}^1_{44}\beta_n^2-\bar{\varsigma}^1_{55}\alpha_m^2-\left(\frac{\tilde{\varsigma}^1_{22}}{R_\beta}\right),\qquad \mathcal{K}_{14}=-\bar{\varsigma}^2_{11}\alpha_m^2-\tilde{\varsigma}^2_{66}\beta_n^2,\qquad \mathcal{K}_{24}=-(\varsigma^2_{12}+\varsigma^2_{66})\alpha_m\beta_n\,,$$

$$\mathcal{K}_{34}=\left(-\bar{\varsigma}^1_{55}+\frac{\varsigma^2_{12}}{R_\beta}\right)\alpha_m,\quad \mathcal{K}_{44}=-\bar{\varsigma}^1_{55}-\bar{\varsigma}^3_{11}\alpha_m^2-\tilde{\varsigma}^3_{66}\beta_n^2,\quad \mathcal{K}_{15}=-(\varsigma^2_{12}+\varsigma^2_{66})\alpha_m\beta_n\,,\quad \mathcal{K}_{25}=-\tilde{\varsigma}^2_{22}\beta_n^2-\bar{\varsigma}^2_{66}\alpha_m^2+\frac{\tilde{\varsigma}^1_{44}}{R_\beta}$$

$$\mathcal{K}_{35}=\left(-\tilde{\varsigma}^1_{44}+\frac{\tilde{\varsigma}^2_{22}}{R_\beta}\right)\beta_n\,,\quad \mathcal{K}_{45}=-(\varsigma^3_{12}+\varsigma^3_{66})\alpha_m\beta_n\,,\qquad \mathcal{K}_{55}=-\tilde{\varsigma}^1_{44}-\bar{\varsigma}^3_{66}\alpha_m^2-\tilde{\varsigma}^3_{22}\beta_n^2.$$

The mass matrix is diagonally by $\bar{I}_1$, $\bar{I}_2$, and $\bar{I}_3$ which are the inertia terms and could defined as:

$$\bar{I}_j=\left[I_j+\frac{I_{j+1}}{R_\beta}\right],\ for\ j=1,2,3,\quad \text{and}\ [I_1,I_2,I_3,I_4]=\sum_{k=1}^{N}\int_{h_{k-1}}^{h_k} I^k\,(1,\zeta,\zeta^2,\zeta^3,\zeta^4)d\zeta,$$

where $I^k$ is the mass density of the k[th] layer of the shell per unit mid-surface area.

## Results and Discussion

Although the proposed ball joint pipe comprises other elements, the current analysis will emphases on the design parameters of the pipe segments only. Based on the thick laminated composite cylindrical shell theory, the transvers stress is simulated a cross the thickness of the pipe segment examining various orthotropy ratio. Figure 2, displays that the transvers stress of laminated composite with weak orthotropy ratio could expand the pipe life. That's obvious, because the pipe properties in the hope direction almost equal to those in longitudinal direction. Results reveal that constructing the pipe segment by composing more layers at cross ply scheme could give similar behavior to those of weak orthotropy ratio.

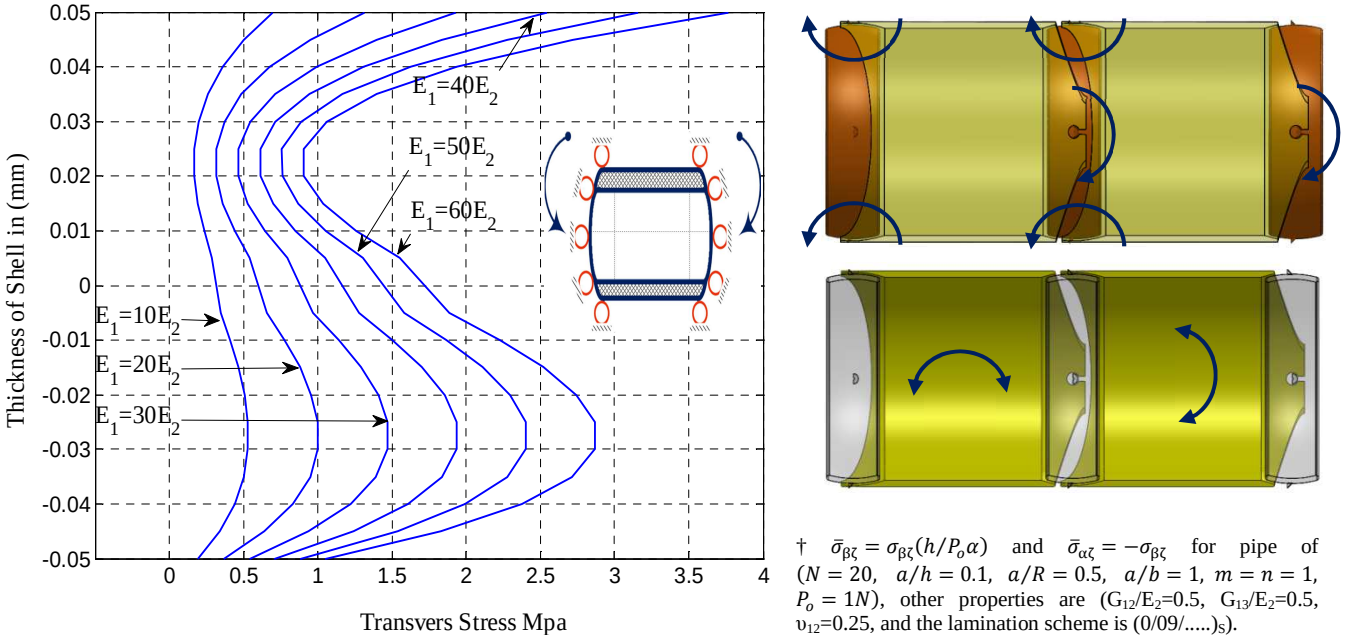


† $\bar{\sigma}_{\beta\zeta}=\sigma_{\beta\zeta}(h/P_o\alpha)$ and $\bar{\sigma}_{\alpha\zeta}=-\sigma_{\beta\zeta}$ for pipe of $(N=20,\ a/h=0.1,\ a/R=0.5,\ a/b=1,\ m=n=1,\ P_o=1N)$, other properties are ($G_{12}/E_2$=0.5, $G_{13}/E_2$=0.5, $\upsilon_{12}$=0.25, and the lamination scheme is $(0/09/.....)_S$).

**Figure 2. The inter-laminar stresses that induced into the pipe segment at diffrent stiffness ratio.**

## Conclusions

In the present work the elastic deformations capacity under pure bending conditions (e.g., typical reeling installation conditions) of ball joint pipe has been analyzed from a theoretical standpoint by means of a physically intuitive treatment. It has been shown that the proposed formulation, which partially attains some classical expressions by a different line of reasoning, is may serve as a reference in designing the composite ball joint pipe and improve the standards and specifications on the flexible pipes. Apart from possessing a clear physical meaning, on account of its simplicity the presented treatment seems also very suitable for developing and prototyping purposes.

## Acknowledgments

The authors would like to acknowledge Universiti Teknologi PETRONAS, Malaysia for sponsoring this research work.

## References

1. Qatu M.S., *Vibration of Laminated Shells and Plates*. 2004, London: Elsevier.
2. Reddy J.N., *Mechanics of Laminated Composite Plates and Shells*. 2004, New York: CRC Press.